GIS Odyssey Journal

2026 • Volume 6 • Number 2

https://doi.org/10.57599/gisoj.2026.6.2.221

Sahil S. Mahamune[1],Nitin L. Gavankar[2]

INTEGRATED ASSESSMENT OF URBAN GROWTH, LAND USE/ LAND COVER DYNAMICS, AND URBAN HEAT ISLAND VARIATIONS USING RANDOM FOREST CLASSIFIER

Abstract: Urbanization significantly leads to changes in Land Use Land Cover (LULC) patterns, LST and Urban Heat Island intensity. This study analyzes the spatio temporal dynamics of LULC, LST and urban growth in Pune-Pimpri-Hinjewadi area over 25 year period (2000 to 2025) using multi temporal Landsat imagery. LULC classification is performed using Random Forest algorithm over four LULC classes (Water, Built-up, Barren, Vegetation). The classification accuracy achieved is in between 84% to 87% with strong Kappa coefficients between 0.78 and 0.83. The built-up increased from 158.88 km^2 in 2000 to 201.94 km^2 in 2025. In addition, Land Surface Temperature (LST) analysis indicates increasing temperature with mean temperatures ranging from 34.36°C (2000) to 45.21°C (2020), while minimum and maximum LST values varied between 18.90–28.53°C and 50.94–74.51°C, respectively. The linear regression relationship between the Normalized Difference Built-up Index (NDBI) and LST showed strong positive correlation ranging from (R^2 = 0.446–0.605). This confirms the impact of urbanization on thermal characteristics. Directional analysis reveals uneven urban growth the northwest (NW) and west (W) zones experiencing the highest growth, while the southeast (SE) zone remained nearly saturated.

Keywords: urban heat islands, spatio temporal, LULC, LST, urban sprawl

Received: 16 June 2026; accepted: 17 August 2026; revised: 12 September 2026

[1] Walchand College of Engineering, Department of Computer Science and Engineering, Sangli, Maharashtra, India, ORCID ID: https://orcid.org/0009-0009-9232-6289, email: sahilmahamune007@gmail.com

[2] Walchand College of Engineering, Department of Computer Science and Engineering, Sangli, Maharashtra, India, ORCID: https://orcid.org/0000-0002-8511-5143, email: nitin.gavankar@walchandsangli.ac.in

Introduction

Since the beginning of human civilization on this earth deforestation, agricultural land changes, expansion of urban area have changed the spatio temporal dynamics of the earth surface. LULC and LST helps to identify the changes caused by the human environment interaction. In recent decades, rapid urbanization and LULC transformation have emerged as dominant drivers. Remote Sensing has become an indispensable tool for analyzing spatio temporal variations in LULC and LST. Urbanization has been widely recognized as a dominant force, shaping land use dynamics, ecological processes, and socio-economic transitions. (Beckers et al., 2020) studied urban expansion in Belgium using cellular automata and agent based agricultural models, revealing significant farmland reduction and farming decline, particularly in peri-urban areas. Large scale land transformation studies provide empirical evidence of spatial change. (Piao et al., 2021) mapped long term land cover change in North Korea using multi temporal Landsat imagery processed with Google Earth Engine and Random Forest classification. The results showed substantial forest recovery. Similarly, Short term environmental responses to human activity were explored by (Guha & Govil, 2021), who analyzed COVID-19 lockdown effects in Raipur using Landsat's thermal and NDVI datasets. The results showed temporary cooling and vegetation recovery. Methodological refinement in land cover estimation was demonstrated by (Sales et al., 2021), who compared pixel count and probability based area estimation using Random Forest outputs were derived from Landsat imagery. Probability based methods improved the classification accuracy. (Sarif & Gupta, 2021) analyzed Prayagraj region using multi temporal Landsat and landscape metrics, identifying dominant edge expansion, while (Baqa et al., 2021) modelled Karachi's growth using Random Forest and CA Markov simulation, predicting continued built-up expansion replacing agricultural land.

Dou & Han (2021) analyzed urban expansion in Dongguan using multi temporal LULC maps on Google Earth Engine, revealing rapid built-up growth and decline in agricultural land. Urban heat and environmental dynamics form another major research focus (Mohammad & Goswami, 2022) analyzed heat and cool island behavior in Indian metropolitan regions using MODIS land surface temperature and environmental indicators, identifying evapotranspiration and thermal inertia as key drivers. (Tariq et al., 2022) linked land surface temperature change to cropping pattern shifts in Hafizabad using Landsat classification and regression analysis, revealing temperature driven agricultural change in many areas of Hafizabad but limited temporal resolution affected the study. (Tariq et al., 2022) another study on Peshawar done using Land Change Modeler and CA Markov simulation to project continued urban expansion, though predictions depended on past transition stability. The study showed 16.3% increase in urban area. (Pandey et al., 2024) showed how built-up increases temperature in Imphal using multi temporal Landsat mapping, but seasonal variability influenced temperature results obtained for the same region. (Tariq & Mumtaz, 2022) similarly demonstrated strong correlation between urban expansion and thermal intensification in Lahore through CA Markov modelling, strong relation in urban expansion and temperature increase was observed. Urban thermal impacts have been observed globally (Kwofie et al., 2022) which demonstrated strong positive relationships between impervious surfaces and temperature in Greater Accra using Landsat and machine learning classification. (Saha et al., 2024) reported increasing seasonal temperature in various areas of Bangladesh associated with urban expansion and deforestation through Landsat satellite data, while (Rendana et al., 2023) linked built-up growth to mangrove degradation through NDVI, NDBI, and LST analysis.

Stability of index temperature relationships was explored by (Guha & Govil, 2025), who focused on the relationship of LST and LULC indices. The pearson's linear correlation coefficient method was applied in determining the correlation analysis. Advances in temperature retrieval and modelling continue to improve monitoring accuracy (Wang et al., 2023) developed a radiance based split window algorithm for Landsat 9 using simulated atmospheric and emissivity datasets which improved accuracy but requires precise parameter inputs. UHI intensification has been documented by many researchers. Siswanto et al. (2023) analyzed Jakarta using Landsat, MODIS, and meteorological data, showing rising heat intensity associated with vegetation loss. Results reported shows that the SUHI intensity is approximately 3°C to 6°C and AUHI is approximately 1°C to 2.5°C. (Jaber & Sengupta, 2024) examined temperature variability in Arid regions using global climate datasets and spatial regression, revealing strong seasonal interactions. (Kaur et al., 2023) monitored land surface changes in the East Godavari region using GEE and Landsat datasets, revealed major LULC changes in forest areas and helped in sustainable land use planning through accurate forest cover analysis. (Phinzi et al., 2023) showed that with larger training datasets using SPOT-7 imagery and Random Forest modelling the accuracy increased. (Wei et al., 2023) used GF-6 satellite for accurate (LULC) classification in urban areas. Feature selection techniques like Minimum Redundancy Maximum Relevance (MRMR) and ML models such as Random Forest and XGBoost demonstrate high classification accuracy. (Krivoguz et al., 2023) found Deep Neural Network and Random Forest demonstrated higher accuracy compared to SVM and AdaBoost. These approaches highlight the effectiveness of advanced algorithms to improve classification performance.

In index based environmental analysis (Tiwari & Kanchan, 2024) demonstrated strong built-up temperature relationships in Varanasi using Landsat correlation analysis. Debnath et al. (2025) observed similar relationships in mountainous terrain, while (Pandey et al., 2025) showed seasonal variation in index–temperature interactions. Urban sprawl structural evolution has also been studied using entropy and spatial metrics. (Barman et al., 2024) analyzed urban expansion using multi temporal Landsat based LULC change detection. Urban sprawl was assessed through Shannon's entropy, landscape metrics, and MLC. The study showed significant urban growth and landscape fragmentation, highlighting the need for sustainable urban planning and controlled development. While (Verma et al., 2024) identified leapfrog growth in Sonipat Kundli using Shannon entropy modelling. (Khan et al., 2024) showed significant built-up expansion and 11°C temperature increase in Aligarh using Landsat classification and thermal analysis. Recent advances focus on improving temperature retrieval and spatial modelling. Li et al. (2025) enhanced ASTER temperature retrieval using XGBoost and TIR data and Splits window algorithm, achieved high quality of LST. Yuan et al. (2025) used Landsat 9 and Sentinel 2 data with machine learning techniques such as XGBoost, Random Forest, and Spatial Random Forest (SRF) to improve LST downscaling accuracy and handle spatial heterogeneity. SHAP was integrated to enhance feature selection and model interpretability.

Predictive urban modelling continues to evolve, (Khan & Khan, 2025) simulated future land and temperature change in Lucknow using CA-ANN modelling, projecting intensified urban heat island effects dependent on obtained historical transition. Zhang et al. (2025) documented severe heat stress increase in Lahore region using long term Landsat and thermal indices, though results heavily dependent on classification accuracy and quality of data obtained. (Zwolska et al., 2025) observed increased heat island intensity in Poznań using Local Climate Zone classification and SUHI for year 1980 and 2020 with the help of Landsat satellite data. Fauzi et al. (2025) analyzed Jakarta's temperature profiles using land cover and albedo data, showing strong relationships between surface properties and air temperature under tropical conditions. (Egziabher et al., 2025) assessed socio-economic impacts of expansion in Ethiopian towns using Landsat change detection and household surveys, identifying agricultural loss and livelihood transitions dependent on governance conditions.

Despite these advancements, many studies have examined LULC changes, urban growth, and LST variations independently, with limited integration of these components over long temporal scales. This gap restricts a complete knowledge of the effects of urbanization on thermal environments. The present study contributes the integrated analytical approach to analyze the interaction between LULC, LST and urban growth dynamics. The main objectives of this study is to extract the urban growth in the study area through LULC classification and using machine learning Algorithm. Further the extracted urban growth has been validated by analyzing change in the Land Surface Temperature and correlating it with NDBI. In order to further validate urban growth, Urban Heat Islands have been calculated, which clearly shows the increase in temperature where urban growth is identified. Thereafter, in order to identify the way urban sprawl expanded, a very important directional urban growth analysis has been carried out, which not only gives an idea about the direction in which urban growth is expanding but also helps in planning and availing socio-economic facilities in the region.

Material and methods

Study area. Pune, the fastest growing metropolitan district in western India, is a major economic, educational, and technological hub of Maharashtra. The Pune–Pimpri–Hinjewadi region has experienced rapid urban expansion in last two and half decades due to industrial sector, IT sector growth, and infrastructural developments. Fig. 1 shows study area which includes Pune-Pimpri-Chinchwad, and Hinjewadi IT corridor along with surrounding peri-urban regions. The selected study area, which spans over 490 km^2. The area, which is located in UTM Zone 43 North (WGS 84 datum), is ideal for studying the dynamics of land surface temperature and urban expansion.

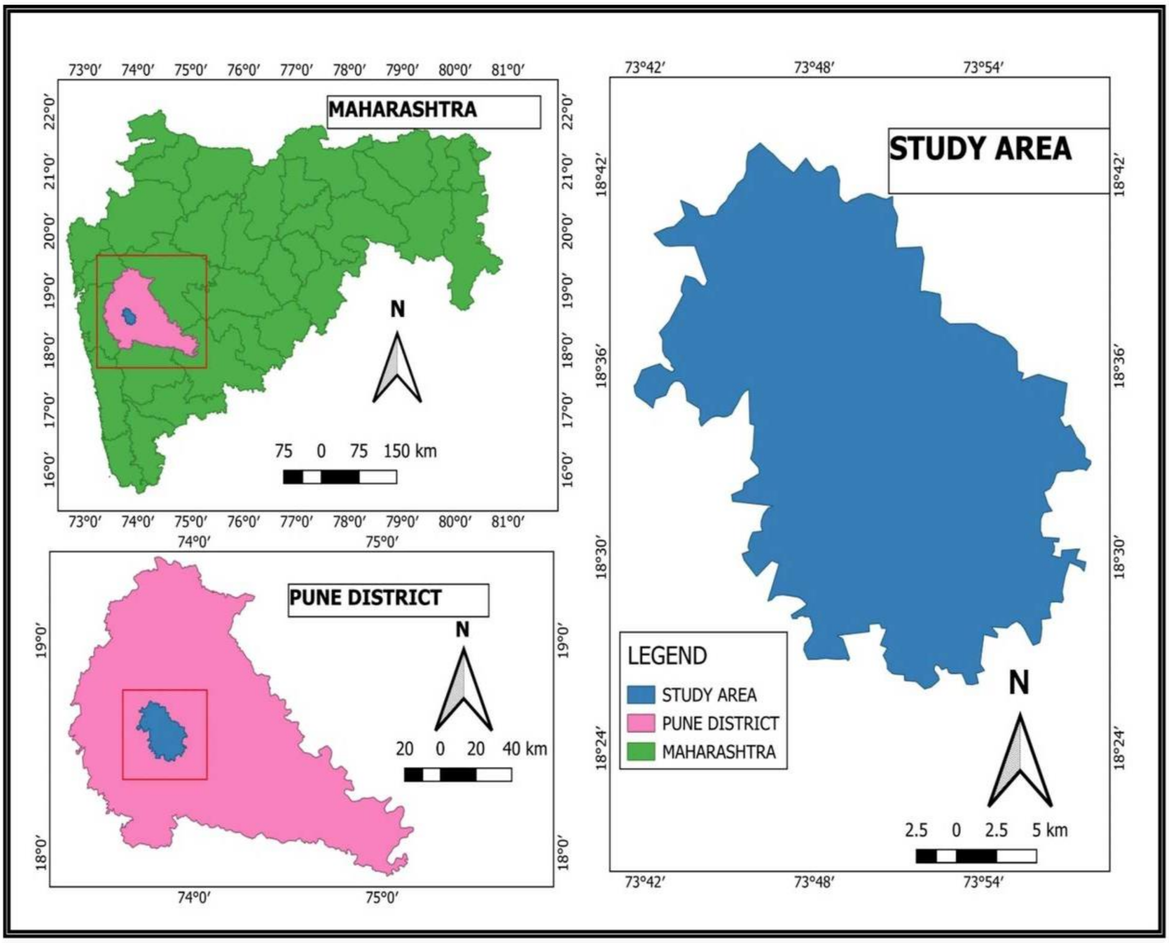

Fig. 1. Study area (Pune-Pimpri-Hinjewadi)
Source: own elaboration

Data acquisition and image preprocessing. Table 1 shows multi temporal satellite imagery acquired to analyze LULC dynamics, changes in LST and LULC indices. In this study Level -2 Landsat satellite data have been used for six distinct years 2000, 2005, 2010, 2015, 2020, and 2025 because of its moderate spatial resolution (30m) and long term continuity. This Level 2 data provides surface temperature (ST) and surface reflectance (SR) data that have been atmospherically adjusted. The image preprocessing shown in Fig. 2 was carried out primarily using ArcGIS pro. The layer stacking was done to combine bands and form composite image. Landsat 7 imagery for 2000, 2005, and 2010 contained SLC off gaps, which were corrected using interpolation techniques to reconstruct missing pixels. After that, images were clipped to fit into the Area of Interest including Pune-Pimpri-Hinjewadi area. This step reduced the data volume and focused the analysis to the study region.

Table 1. Satellite data used for LULC, LST and urban sprawl

Years	Acquisition Date	Satellite
2000	2/2/2000	Landsat 7
2005	3/3/2005	Landsat 7
2010	17/3/2010	Landsat 7
2015	7/3/2015	Landsat 8
2020	20/3/2020	Landsat 8
2025	10/3/2025	Landsat 9

Source: own elaboration

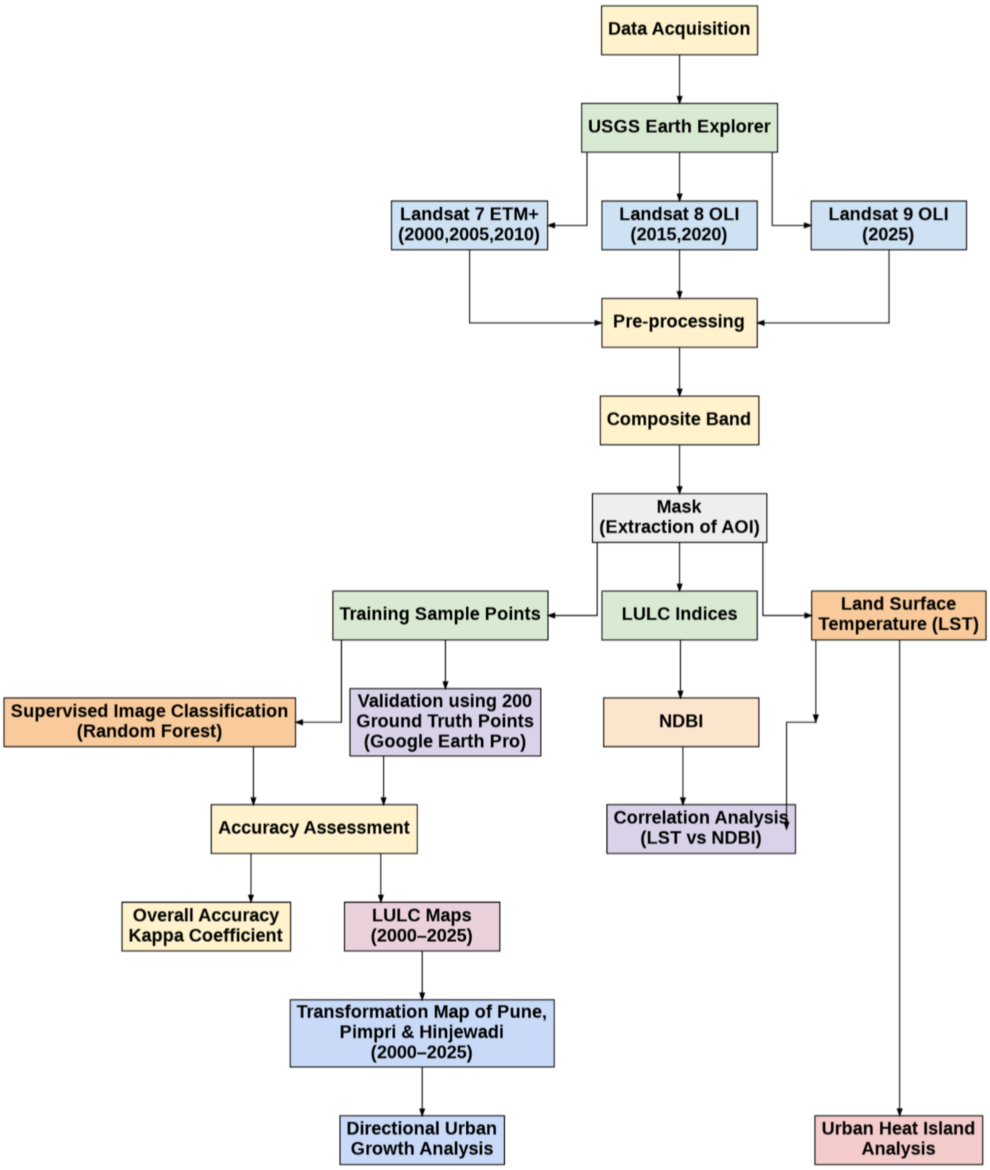

Fig. 2. Flow diagram of proposed methodology
Source: own elaboration

LULC classification and accuracy assessment. Here, in this study supervised image classification is performed on the processed and composite images. According to Barman et al. (2024), supervised classification is a method that uses training samples with labeled land cover to classify image pixels according to their spectral signatures. The Random Forest (RF) technique in ArcGIS pro is use for categorization in this work (Sales et al., 2021; Baqa et al., 2021; Wei et al., 2023). Random forest is the ensemble based ML technique it consists of multiple decision trees which helps to get high accuracy. Total 4400 training samples were generated and equally distributed among four major LULC classes. The spectral signatures were extracted from the clipped AOI of six different years and classification was carried out. After that accuracy analysis was carried out. For accuracy analysis, total of 200 random validation points were considered separately for each year and they were independent of training samples. Google Earth Pro's high resolution imagery was used to verify these points (Khan & Khan, 2025, Guha & Govil, 2025). Further, a confusion matrix is use to evaluate the validity of the classification. The parameters such as, Producer's Accuracy, User's Accuracy, Overall Accuracy, and Kappa Coefficient were obtained using eq. 1, 2, 3, and 4 respectively (Tariq & Mumtaz, 2023; Zafar et al., 2024).

$$Producer's\ Accuracy = \frac{\text{Correctly Classified pixels}}{\text{Total Reference Pixels}} \times 100 \tag{1}$$

$$User's\ Accuracy = \frac{\text{Correctly Classified pixels}}{\text{Total Classified Pixels}} \times 100 \tag{2}$$

$$Overall\ Accuracy = \frac{\text{Total Correct Classifications}}{\text{Total Number of Samples}} \times 100 \tag{3}$$

$$Kappa\ Coefficient = \frac{(\mathrm{N} * \sum \mathrm{X_{ii}} - \sum(\mathrm{X_{i+}} * \mathrm{X_{+i}}))}{(\mathrm{N}^2 - \sum(\mathrm{X_{i+}} * \mathrm{X_{+i}}))} \tag{4}$$

Estimation of LST. The primary metric for examining the thermal properties of the earth's surface is land surface temperature (LST). Since it offers continuous spatial temperature information across extensive areas, remote sensing based LST retrieval has gained widespread acceptance (Kazemi et al., 2025). Level-2 Landsat data, which offers atmospherically adjusted data, is being use in this study to calculate LST. Landsat 7's band 6 and Landsat 8's band 10 were used to acquire LST. The standard scaling eq. 5,6 are used to transform the pixel values into temperature (Zwolska et al., 2025).

$$LST(K) = (\text{ST\_Band} * 0.00341802) + 149.0 \tag{5}$$

The results were converted from kelvin to Celsius.

$$LST(°\text{C}) = LST(K) - 273.15 \tag{6}$$

Previous studies have shown LST as strongly influenced by land use patterns. Built-up areas tend to exhibit higher temperatures, while vegetation and water bodies contribute to cooling effects (Debnath et al., 2025). Multi temporal Landsat data have been effectively used to analyze such relationships between urban growth and temperature rise (Khan and Khan 2025). From the derived LST maps for all study years during 2000–2025 mean LST was calculated for each LULC class and high temperature zones were compared with built-up areas.

Calculation of LULC indices and relationship between LST and NDBI. Different LULC indices like NDBI, NDVI, and MNDWI are important for extracting vegetation, Built-up, water bodies (Tiwari and Kanchan 2024, Khan and Khan 2025, Guha and Govil 2025). Table 2 shows the required bands. Such as NIR and Red bands for NDVI, Green and Shortwave Infrared 1 (SWIR 1) for MNDWI and SWIR 1 and NIR for NDBI (Tariq & Mumtaz, 2020; Kwofie et al., 2022).

To analyze urbanization effects on surface thermal properties, the relation between LST and NDBI is examined (Debnath et al., 2025; Khan & Khan, 2025; Pandey et al., 2025). To analyze the correlation between LST and NDBI. Total 200 points were considered randomly across study area to extract corresponding pixel values of LST and NDBI. Linear regression analysis was performed to measure the strength and direction of correlation between the two variables.

Table 2. LULC indices formula

LULC Indices	Formula
Normalized Difference Vegetation Index (NDVI) (Tariq and Mumtaz 2022)	$NDVI = \frac{NIR - RED}{NIR + RED}$
Normalized Difference Built-up Index (NDBI) (Tariq and Mumtaz 2022)	$NDBI = \frac{SWIR - NIR}{SWIR + NIR}$
Modified Normalized Difference Water Index (MNDWI) (Kwofie et al. 2022)	$MNDWI = \frac{GREEN - SWIR}{GREEN + SWIR}$

Source: own elaboration

Directional analysis of built-up expansion. To understand the urban expansion pattern a directional spread analysis was performed with respect to the city center of the study area. Urban growth generally occurs outside the city center therefore, inspecting the expansion in different directions provides insights of dominant growth trends. The entire study area was split up into eight directional zones using the ArcGIS directional tool, and measuring the total area the city centre was plotted which serve as the point of reference. The directional analysis of Built-up area was carried out for year 2000 and 2025 and was measured in km². This directional analysis provided a clear understanding of how urbanization has progressed from central core to different direction of study area.

Results

Spatio temporal LULC changes and accuracy assessment. Here in this study the Random Forest Algorithm shows the significant changes in all four LULC classes shown in Table 3 and (Fig. 3 a-f). However, among all classes the built-up area increased from 158.88 km^2 in 2000 to 201.94 km^2 in 2025, this indicates rapid growth and infrastructure development Fig. 3a and Fig. 3f. On the other hand, barren land decrease from 244.14 km^2 in 2000 to 186.45 km^2 in 2025 suggesting conversion of unused land into built-up areas. However, after 2005 the vegetation cover seen relatively stable at and around 97 to 99 km^2 showing no much change in vegetation cover. Similarly, water bodies showed minimal variations decreasing from 6.96 km^2 in 2000 to 6.57 km^2 in 2025.

Table 3. Spatio temporal changes in LULC from 2000–2025

Years	Barren (km^2)	Built-up (km^2)	Vegetation (km^2)	Water (km^2)
2000	244.14	158.88	80.06	6.96
2005	219.57	166.66	96.90	6.85
2010	208.84	177.67	96.77	6.72
2015	203.94	182.33	96.00	6.70
2020	194.70	188.84	99.88	6.59
2025	186.45	201.94	95.06	6.57

Source: own elaboration

Additionally, to validate the categorized (LULC) maps, an accuracy assessment is conducted utilizing 200 reference points from Google Earth Pro imagery for each study year. During accuracy assessment, these validation points were compared with classified outputs and overall accuracy along with kappa coefficient were calculated using the formulas shown in eq. 3 and eq. 4. The classified maps achieved overall accuracy ranging from 84% to 87% for years 2000 to 2025. Similarly, the kappa coefficient values obtained are in the range from 0.78 to 0.83 shown in Table 4. Which indicates a good agreement between classified images and validation points. Further, this major spatio temporal changes in LULC may have also caused thermal changes in study area. Therefore, in order to analyse the impact of this Land cover transformation on urban thermal conditions, LST analysis has been carried out.

Table 4. Classification accuracy and kappa coefficient

Years	Overall Accuracy (%)	Kappa Coefficient
2000	86	0.81
2005	84.5	0.79
2010	86	0.81
2015	86.5	0.82
2020	84	0.78
2025	87	0.83

Source: own elaboration

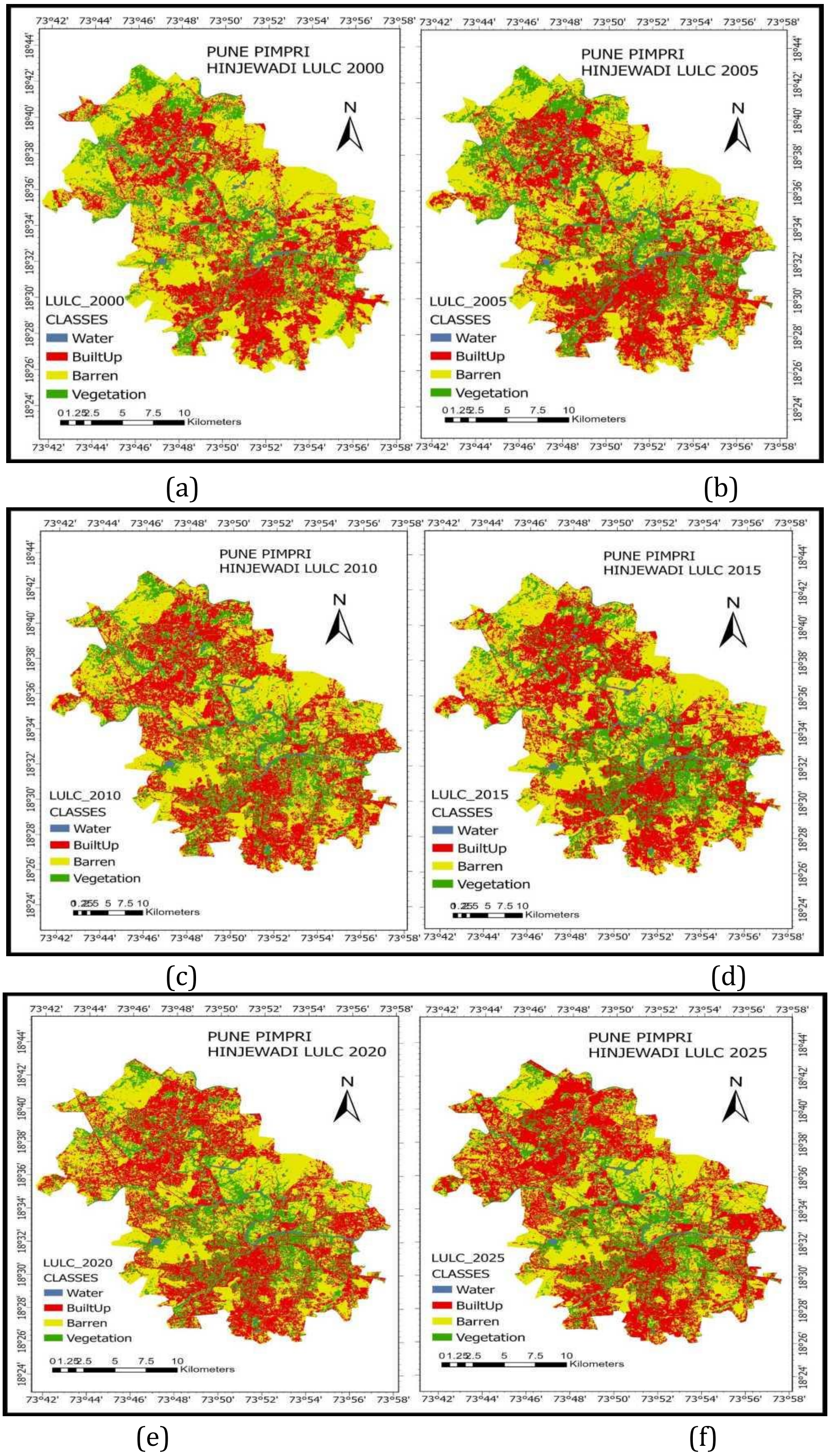

Fig. 3. Land Use Land Cover map of Pune-Pimpri-Hinjewadi for years
(a) 2000 (b) 2005 (c) 2010 (d) 2015 (e) 2020 and (f) 2025
Source: own elaboration

Land surface temperature variations in study area. To understand the thermal dynamics of the study area, the shifts in LST as shown in Table 5 from year 2000 to 2025 were examined for Pune-Pimpri-Hinjewadi region. The minimum LST increased from 19.93°C in 2000 to 28.53 °C in 2020 and the small decrease to 27.34°C in 2025. Indicating the overall warming trend in the study area. (Fig. 4a–f) shows the gradual increase in hot area from 2000 to 2025. In addition, mean LST shows increasing trend from 34.36°C in 2000 to 45.21°C in 2020. The rise in minimum and mean temperature indicates the change in UHI. Further, to examine which LULC class is influencing the rise in temperature and understanding how different LULC classes affect the surface thermal behavior a comparative analysis of LST across different LULC classes is done.

Table 5. Land Surface Temperature from 2000–2025

Land Surface Temperature (◦C)			
Years	Minimum	Maximum	Mean
2000	19.93	74.51	34.36
2005	18.90	56.48	40.89
2010	19.64	57.49	42.86
2015	26.49	50.94	38.67
2020	28.53	58.71	45.21
2025	27.34	53.78	40.38

Source: own elaboration

Comparative analysis of LST and different LULC classes. The analysis of LST across various LULC classes is perform to examine variations in thermal behavior of different classes Fig. 5. The comparative analysis shows clear differences in mean temperature among all land cover classes, wherein Barren land and Built-Up classes consistently exhibiting the highest LST. In 2010 the built-up area observed 42.22°C of mean LST and it increased to 45.14°C in 2020.Similarly the barren land also showed the rise of temperature from 45.40°C in 2010 to 47.09°C in 2020 Fig. 5. Since, Built-up area showed a strong association with elevated LST, in the next section relationship analysis between LST and spectral indices has been carried out.

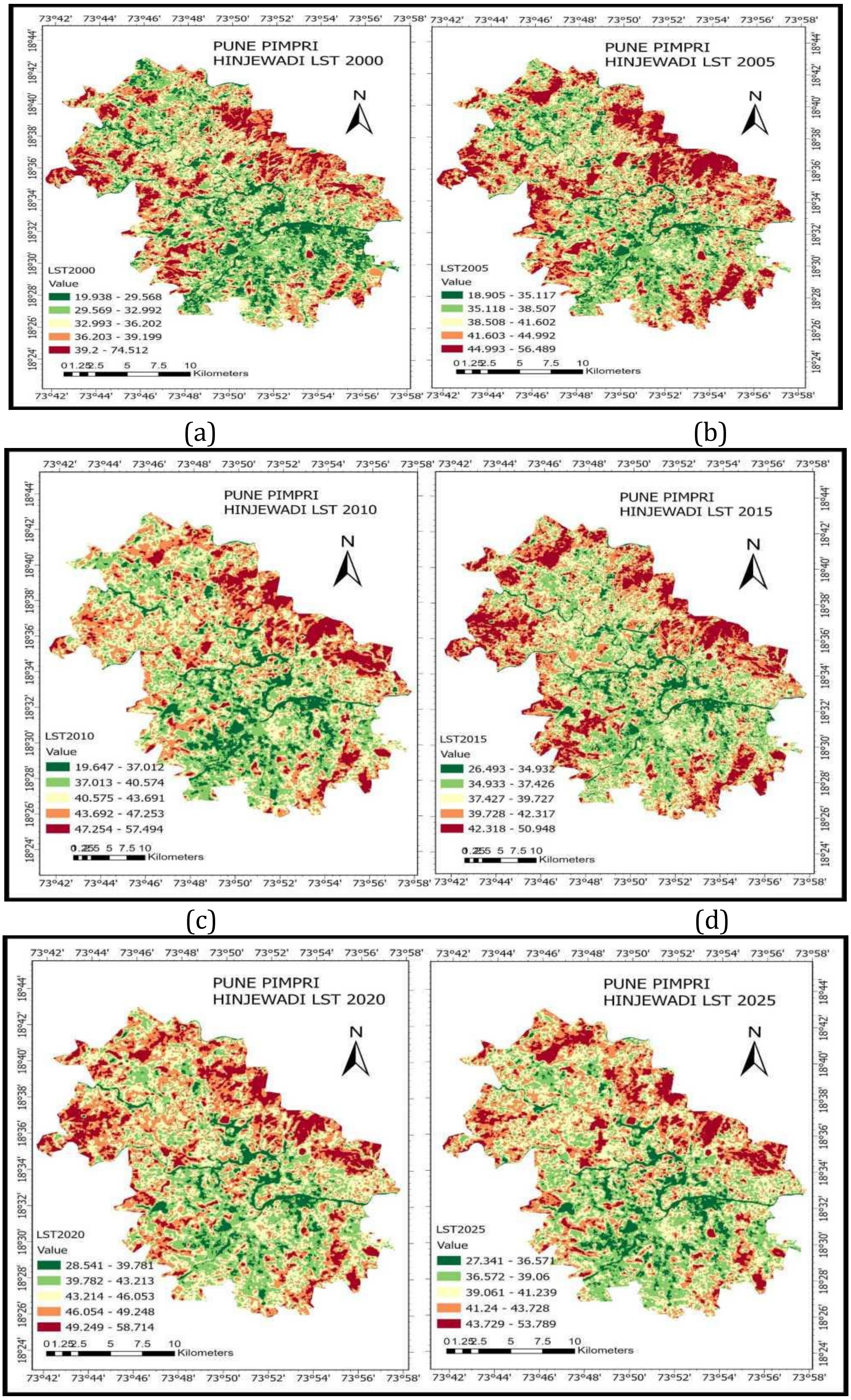

(a) (b)

(c) (d)

(e) (f)

Fig. 4. Land Surface Temperature map of Pune-Pimpri-Hinjewadi for years (a) 2000 (b) 2005 (c) 2010 (d) 2015 (e) 2020 and (f) 2025
Source: own elaboration

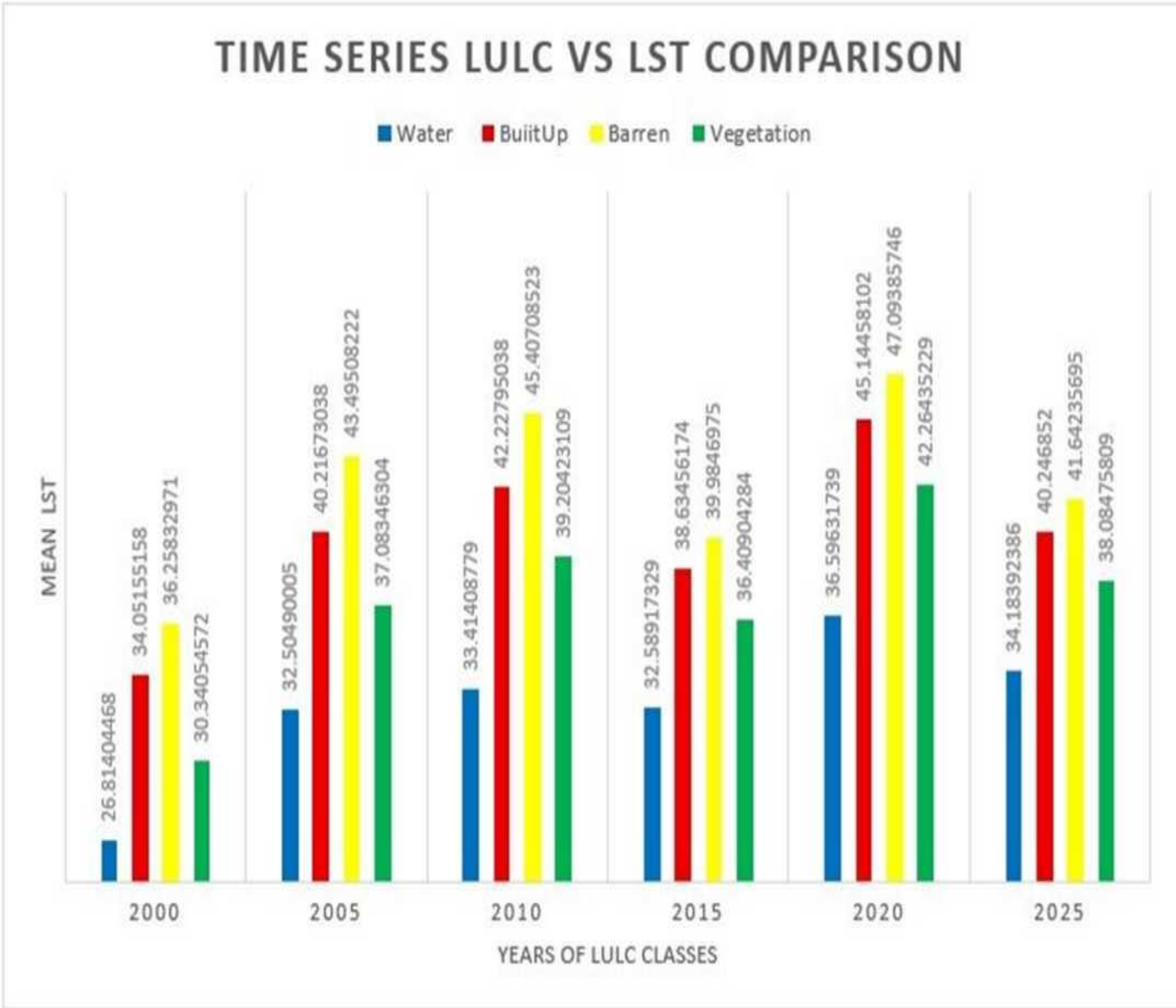

Fig. 5. Class wise Mean LST from year 2000 to 2025
Source: own elaboration

Relationship between LST and NDBI. The relationship between LST and NDBI is analyzed using Linear Regression from year 2000 to 2025 shown in (Fig. 6a-f), these Figures represent the values of NDBI and LST using 200 random points. The strength of the correlation among built-up area and surface temperature is rated using R^2 values shown in Table 6. The R^2 value in 2000 was 0.446, suggesting a robust correlation between LST and NDBI. In 2005 the R^2 values increased to 0.58, showing stronger correlation, the peak strength was observed in 2010 with R^2 value of 0.605, indicating strongest correlation among all years. The above analysis demonstrate that built-up areas play a crucial role in increasing land surface temperature. So, to analyze whether urban growth is uniform or not and to analyze its intensity the directional study of urban growth was carried out.

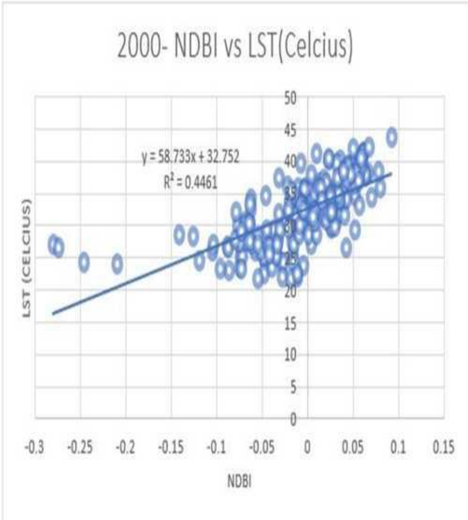

(a)

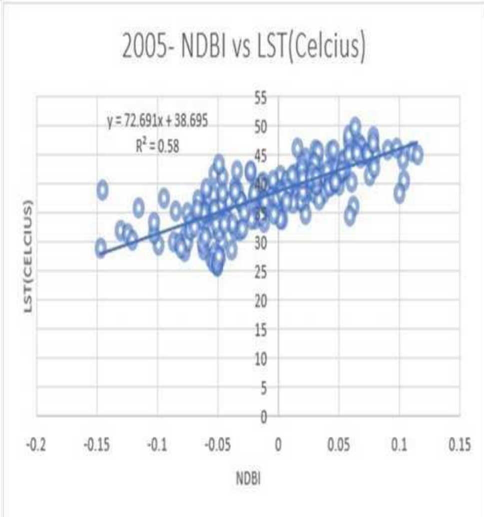

(b)

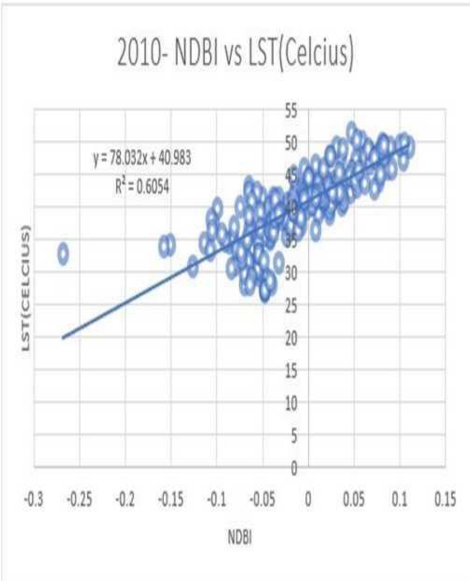

(c)

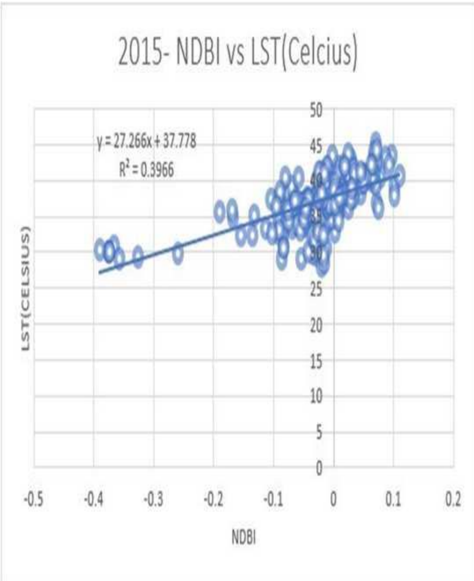

(d)

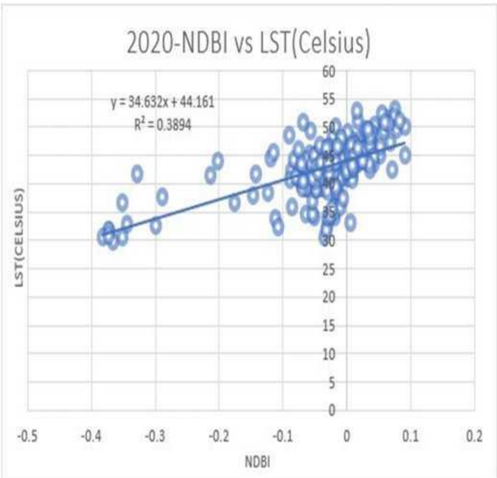

(e)

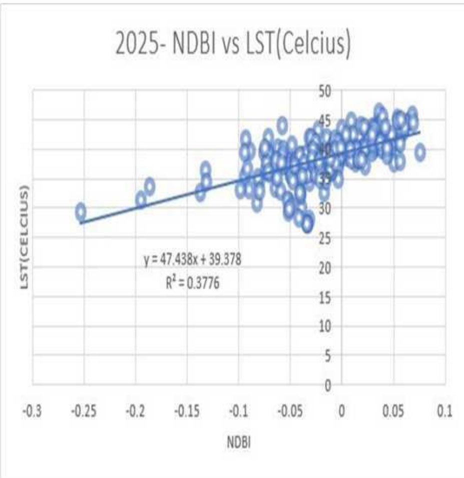

(f)

Fig. 6. LST vs NDBI correlation analysis for years
(a) 2000 (b) 2005 (c) 2010 (d) 2015 (e) 2020 and (f) 2025
Source: own elaboration

Table 6. Linear regression correlation between LST and NDBI from 2000–2025

Years	R^2 values	Interpretation
2000	0.446	Strong
2005	0.58	Strong
2010	0.605	Strong
2015	0.396	Moderate
2020	0.389	Moderate
2025	0.377	Moderate

Source: own elaboration

Spatio temporal analysis of urban growth and its intensity. The spatio temporal analysis of urban growth is done by analyzing directional growth in urban areas during year 2000 to 2025. The results in Table 7. shows remarkable growth in urban area in study region. Fig. 7a and Fig. 7b. shows that the urban expansion occurred in the study region is not uniform in all directions. However, some zones exhibit higher growth which may be due to available socio-economic facilities and natural ecosystem.

North (N) zone showed moderate urban growth where built-up area increased from 7.7 km^2 in 2000 to 12.74 km^2 in 2025. North zone includes a small part of Bhosari MIDC industrial area which is an important reason for this urban expansion. Similarly, the North East (NE) zone shows slow urban expansion, from 7.3 km^2 in 2000 to 8.9 km^2 in 2025. This may be due to physical constraints. Among all zones the North West (NW) zone experienced the highest urban growth, with built-up area increased from 32.67 km^2 to 46.55 km^2. This maybe due to factors such as Pune Mumbai highway which gives better road connectivity. The West (W) zone also showed remarkable growth from 16.21 km^2 to 34.54 km^2, primarily influenced by the development of the Hinjewadi IT hub.

Table 7. Directional urban growth in year2000 and 2025

Directional Zones	Area in year2000(km^2)	Area in year 2025 (km^2)	Remark
N	7.7	12.74	Moderate
NE	7.3	8.9	Low to moderate
NW	32.67	46.55	High
S	18.67	18.91	Low
SE	40.82	41.21	Saturated
SW	5.9	8.38	Low to moderate
W	16.21	34.54	High
E	27.30	27.58	Low

Source: own elaboration

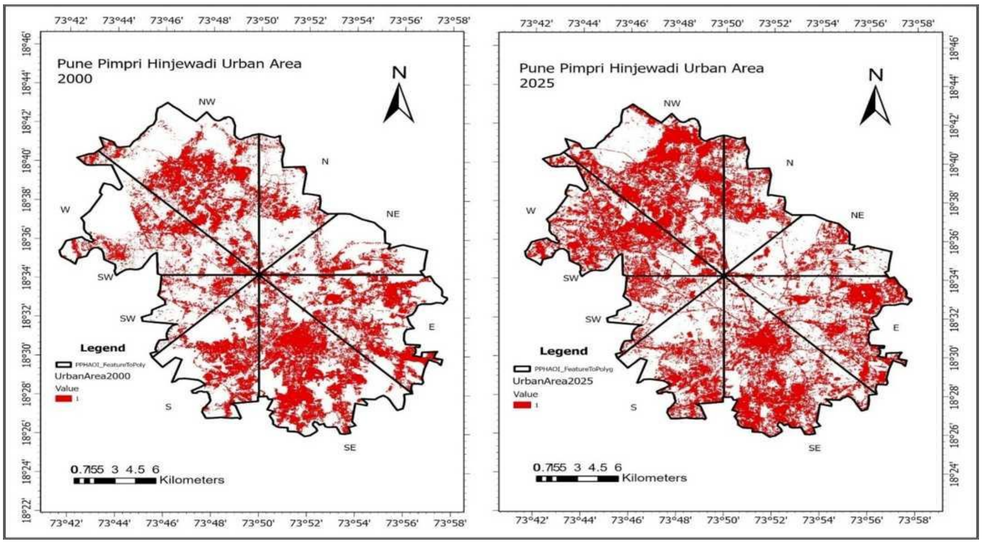

(a) (b)

Fig. 7. Direction wise urban growth from year (a)2000 to (b)2025
Source: own elaboration

The South (S), South East (SE), and East zones showed limited urban growth. South zone contains the mountain and therefore has limited land for built-up. Similarly, the East zone experienced restricted expansion due to military cantonment areas and controlled land use. The South East (SE) zone is one of the most urbanized regions in the study area. The urban area expanded barely from 40.82 km^2 in 2000 to 41.21 km^2 in 2025. The high built-up area in the base year tells that this zone was already highly developed before 2000. The South West (SW) zone shows moderate increase in urban area from 5.9 km^2 in 2000 to 8.38 km^2 in 2025.The growth in this zone is slow but steady indicating future development potential.

Overall, the spatio temporal urban growth analysis revealed that urban expansion in the study area is highly uneven., which may alter surface energy balance and contribute to heat accumulation. This may further cause the development and intensification of the UHI effect. Therefore, to assess the thermal impact of urban growth, the increase in LST and UHI intensity from 2000 to 2025 is analysed in the subsequent section.

Increase in LST and Urban Heat Island intensity from 2000 to 2025. The Spatial distribution of UHI intensity for the years 2000 and 2025 reveals a significant increase in urban surface heating across the study area. Fig. 8a shows UHI for the Year 2000 and Fig. 8b shows UHI for Year 2025. In year 2000 the LST ranged from 19.93°C to 47.85°C where majority of study area is seen under cool and moderate temperature zones and very small area is seen under high temperature hotspots this indicates the lower UHI intensity. However, this scenario completely in year 2025 where LST ranged from 31.80 °C to 52.70 °C. This shows the expansion of high temperature zones and stronger heat concentration this further caused increase in high temperature hotspots across urban areas. The difference between mean LST of year 2000 and 2025 is 6.39°C. This indicates significant intensified UHI over the study period.

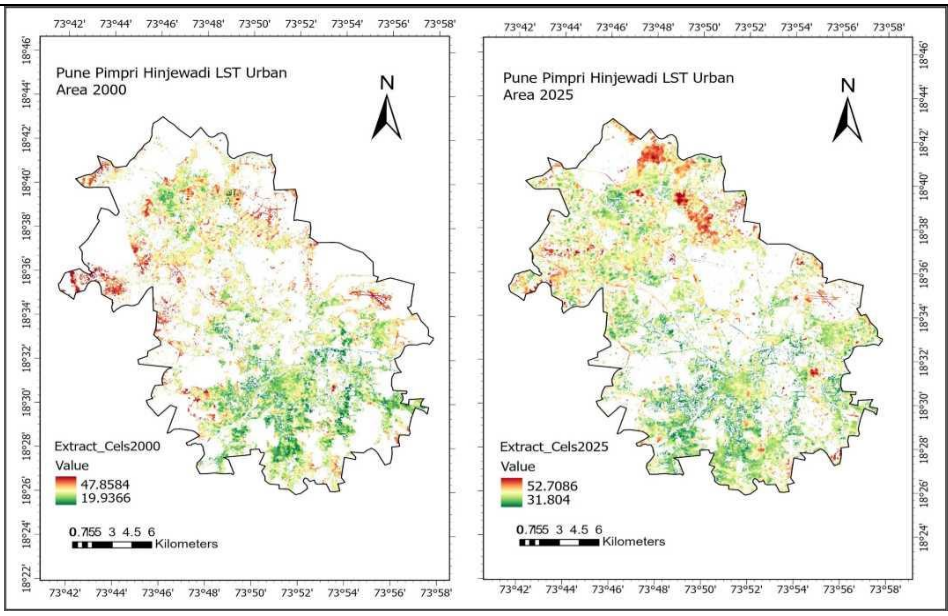

(a) (b)

Fig. 8. Urban Heat Islands from year (a)2000 to (b)2025
Source: own elaboration

Discussion

The current study findings show how urbanization affected the study region's thermal characteristics and land cover dynamics. The LULC spatio temporal study shows a steady rise in built-up during the years 2000 to 2025, decline in barren land and fluctuation in vegetation and water bodies. These transformations are recognized as key drivers of environmental change as urban expansion alters surface characteristics and landscape structure (Sales et al., 2021; Wei et al., 2023). Temporal LST research revealed a significant link between LST and rising built-up. As vegetation and water bodies retain lower temperatures, built-up and barren regions continually display higher LST values. The mean LST exhibits an increasing pattern. This confirms that natural resources helps in cooling the atmosphere whereas more heat is absorbed and retained by concrete and asphalt structures.

The results obtained clearly shows that barren land records the highest temperatures, followed by built-up areas, vegetation, and water bodies respectively as per the class wise LST studies. These findings are in line with the UHI phenomenon, which is characterized by higher temperatures in urbanized areas relative to nearby rural areas as a result of anthropogenic heat emission and land cover changes (Siswanto et al., 2023). The impact of built-up regions over thermal properties is further supported by the relationship between LST and NDBI.

The regression analysis indicates strong correlation which suggests that urban expansion has dominant impact on LST. Similar studies (Debnath et al., 2025; Pandey et al., 2025; Tiwari & Kanchan, 2024) have reported that LST has strong positive relation with built-up indices and negative relation with vegetation and water indices which highlights the role of land cover composition in regulating surface temperature, (Tiwari & Kanchan, 2024). The directional analysis of urban growth reveals that expansion is also not uniform, wherein certain zones, particularly the northwest and west directions, experiencing higher growth intensity. Such spatially uneven urban growth patterns are influenced by infrastructure development, accessibility, and socio-economic facilities in the region, leading to heterogeneous land transformation (Dou & Han, 2022). The outcomes highlight the need for sustainable urban planning strategies, including increasing vegetation cover, preserving water bodies, and promoting environmentally balanced development to mitigate rising temperatures and ensure long term urban sustainability.

Conclusion and future scope

Using multi temporal Landsat data, this research examined LULC, LST, and their relationship with NDBI, over the period of 2000 to 2025. The results show significant changes in the landscape cover and its impact on the thermal climate in the study area. The LULC analysis reveals minimal changes in vegetation and water bodies (5.60%), a gradual decline in barren land (23.63%), and a high (27.10%) expansion of the built-up area during the years 2000 to 2025. The accuracy assessment confirms the reliability of the classification results, with overall accuracy of 87% and strong Kappa coefficient value (0.83). The LST analysis demonstrates a general increasing trend in surface temperature, with peak values observed in the year 2020, indicating intensified thermal conditions. The class wise LST analysis reveals that temperatures are higher in urban areas upto (45.14°C). Further the strong association between LST and NDBI indicates that growing built-up areas are a major factor in rising surface temperatures. The directional analysis further highlights that urban growth is also uneven, wherein certain zones experiencing higher expansion intensity.

In order to improve accuracy, the future studies may concentrate on using satellite data with finer resolution, like sentinel. By combining socio-economic and meteorological data with strong ML and DL algorithms, it is feasible to learn more about urban growth patterns and thermal dynamics. This may improve policy making and sustainable urban planning for government agencies.

Conflict of interest

The authors declare that there are no conflicts of interest. The authors have no financial, personal, academic, or professional relationships that could have influenced the work reported in this paper.

Funding

This research received no specific grant from any funding agency in the public, commercial, or not for profit sectors.

Authors contributions

All authors contributed to the study conception and design. Data collection, preprocessing, analysis, and interpretation were performed by the authors collaboratively. The first draft of the manuscript was written by the first author and both authors reviewed and approved the final manuscript.

Acknowledgement

The authors acknowledge the support of the Department of Computer Science and Engineering and the guidance provided by faculty members during the completion of this research work. Special thanks are extended to all individuals who directly or indirectly contributed to the successful completion of this study.

Ethics approval

This study does not involve human participants, animals, or any confidential data; therefore, ethics approval was not required.

Data availability statement

The datasets used and analyzed during the current study are publicly available from the United States Geological Survey (USGS) Earth Explorer repository and other publicly accessible sources. Processed data generated during the study are available from the corresponding author upon reasonable request.

Use of Generative AI and AI-assisted technologies

No generative AI or AI-assisted technologies were employed in the preparation of this manuscript.

References

Baqa M.F., Chen F., Lu L., Qureshi S., Tariq A., Wang S., Jing L., Hamza S., & Li Q. (2021). Monitoring and modeling the patterns and trends of urban growth using urban sprawl matrix and CA-Markov model: A case study of Karachi, Pakistan. Land, 10(7), 700. https://doi.org/10.3390/land10070700.

Barman S., Roy D., Sarkar B.C., Almohamad H., Abdo H.G. (2024). Assessment of urban growth in relation to urban sprawl using landscape metrics and Shannon's entropy model in Jalpaiguri urban agglomeration, West Bengal, India. Geocarto International, 39(1), 2306258. https://doi.org/10.1080/10106049.2024.2306258.

Beckers V., Poelmans L., Van Rompaey A., Dendoncker N. (2020). The impact of urbanization on agricultural dynamics: A case study in Belgium. Journal of Land Use Science, 15(5), 626–643. https://doi.org/10.1080/1747423X.2020.1769211.

Debnath M., Poddar I., Saha A., Islam N., Roy R. (2025). Analysis of land surface temperature and its correlation with urban, water, vegetation, and surface indices in the Siliguri Urban Agglomeration area of the Himalayan foothill region. Geomatics, Natural Hazards and Risk, 16(1), 2470393. https://doi.org/10.1080/19475705.2025.2470393.

Dou P., Han Z. (2021). Quantifying land use/land cover change and urban expansion in Dongguan, China, from 1987 to 2020. IEEE Journal of Selected Topics in Applied Earth Observations and Remote Sensing, 15, 201–210. https://doi.org/10.1109/JSTARS.2021.3133703.

Egziabher T.G., Gashu K., Mengist D., Maru M. (2025). Urban expansion and its impact on land use/land cover change and the surrounding community in intermediate Ethiopian towns. Urban, Planning and Transport Research, 13(1), 2592418. https://doi.org/10.1080/21650020.2025.2592418.

Fauzi R., Arifin H.S., Perdana P. (2025). Study of urban temperature profiles on various land covers in the Greater Jakarta region, Indonesia. Journal of Natural Resources and Environmental Management, 15(2), 243–244. https://doi.org/10.29244/jpsl.15.2.243.

Guha S., Govil H. (2021). COVID-19 lockdown effect on land surface temperature and normalized difference vegetation index. Geomatics, Natural Hazards and Risk, 12(1), 1082–1100. https://doi.org/10.1080/19475705.2021.1914197.

Guha S., Govil H. (2025). Evaluating the stability of the relationship between land surface temperature and land use/land cover indices: A case study in Hyderabad city, India. Geology, Ecology, and Landscapes, 9(1), 231–243. https://doi.org/10.1080/24749508.2023.2182083.

Jaber S.M., Sengupta R. (2024). Spatial and temporal variabilities in land surface temperatures and near-surface air temperatures in an arid to semiarid urban region: Implications for urban heat island research. Geo-spatial Information Science. https://doi.org/10.1080/10095020.2024.2310589.

Kaur H., Tyagi S., Mehta M., Singh D. (2023). Time series (2001/2002–2021) analysis of Earth observation data using Google Earth Engine (GEE) for detecting changes in land use land cover (LULC) with specific reference to forest cover in East Godavari region, Andhra Pradesh, India. Journal of Earth System Science, 132, 86. https://doi.org/10.1007/s12040-023-02099-w.

Kazemi A., Cirella G.T., Hedayatiaghmashhadi A., Gili M. (2025). Temporal-spatial distribution of surface urban heat island and urban pollution island in an industrial city: Seasonal analysis. IEEE Journal of Selected Topics in Applied Earth Observations and Remote Sensing, 18. https://doi.org/10.1109/JSTARS.2025.3541406.

Khan D., Bano S., Khan N. (2024). Spatio-temporal analysis of urbanization effects: Unravelling land use and land cover dynamics and their influence on land surface temperature in Aligarh City. Geology, Ecology, and Landscapes. https://doi.org/10.1080/24749508.2024.2409488.

Khan D., Khan N. (2025). Modelling urban future: Integrating CA-ANN model for comprehensive understanding of land use, land cover changes, and temperature dynamics in Lucknow City, India. Geology, Ecology, and Landscapes. https://doi.org/10.1080/24749508.2025.2524207.

Krivoguz D., Chernyi S.G., Zinchenko E., Silkin A., Zinchenko A. (2023). Using Landsat-5 for accurate historical LULC classification: A comparison of machine learning models. Data, 8(9), 138. https://doi.org/10.3390/data8090138.

Kwofie S., Nyamekye C., Boamah L.A., Adjei F.O., Arthur R., Agyapong E. (2022). Urban growth nexus to land surface temperature in Ghana. Cogent Engineering, 9(1), 2143045. https://doi.org/10.1080/23311916.2022.2143045.

Li J., Li K., Qian Y., Dou X., Han Q., Zeng J., Zhao H., Lan Q., Xu Z., Bai J., Wei B., Liu X., Wang F., Yang J., Wang Y. (2025). An urban land surface temperature and emissivity separation algorithm from ASTER TIR data and its application. International Journal of Digital Earth, 18(1), 2459346. https://doi.org/10.1080/17538947.2025.2459346.

Mohammad P., Goswami A. (2022). Exploring different indicators for quantifying surface urban heat and cool island together: A case study over two metropolitan cities of India. Environment, Development and Sustainability. https://doi.org/10.1007/s10668-022-02509-x.

Pandey A., Mondal A., Guha S., Upadhyay P.K., Singh D. (2024). Land use status and its impact on land surface temperature in Imphal city, India. Geology, Ecology, and Landscapes, 8(3), 261–275. https://doi.org/10.1080/24749508.2022.2131962.

Pandey A., Mondal A., Guha S., Upadhyay P.K., Rashmi & Kundu S. (2025). Comparing the seasonal relationship of land surface temperature with vegetation indices and other land surface indices. Geology, Ecology, and Landscapes, 9(4), 1211–1227. https://doi.org/10.1080/24749508.2024.2392391.

Phinzi K., Ngetar N.S., Pham Q.B., Chakilu G.G., Szabo S. (2023). Understanding the role of training sample size in the uncertainty of high-resolution LULC mapping using random forest. Earth Science Informatics, 16, 3667–3677. https://doi.org/10.1007/s12145-023-01117-1.

Piao Y., Jeong S., Park S., Lee D. (2021). Analysis of land use and land cover change using time-series data and random forest in North Korea. Remote Sensing, 13(17), 3501. https://doi.org/10.3390/rs13173501.

Rendana M., Idris W.M.R., Abdul Rahim S., Abdo H.G., Almohamad H., Al Dughairi A.A., Albanai J.A. (2023). Effects of the built-up index and land surface temperature on the mangrove area change along the southern Sumatra coast. Forest Science and Technology, 19(3), 179–189. https://doi.org/10.1080/21580103.2023.2220576.

Saha J., Ria S.S., Sultana J., Shima U.A., Seyam M.M.H., Rahman M.M. (2024). Assessing seasonal dynamics of land surface temperature (LST) and land use land cover (LULC) in Bhairab, Kishoreganj, Bangladesh: A geospatial analysis from 2008 to 2023. Case Studies in Chemical and Environmental Engineering, 9, 100560. https://doi.org/10.1016/j.cscee.2023.100560.

Sales M.H.R., de Bruin S., Souza C., Jr. & Herol M. (2021). Land use and land cover area estimates from class membership probability of a random forest classification. IEEE Transactions on Geoscience and Remote Sensing. https://doi.org/10.1109/TGRS.2021.3080083.

Sarif M.O., Gupta R.D. (2021). Modelling of trajectories in urban sprawl types and their dynamics (1988–2018): A case study of Prayagraj City (India). Arabian Journal of Geosciences, 14, 1347. https://doi.org/10.1007/s12517-021-07573-7.

Siswanto S., Nuryanto D.E., Ferdiansyah M.R., Prastiwi A.D., Dewi O.C., Gamal A. (2023). Spatio-temporal characteristics of urban heat island of Jakarta metropolitan. Remote Sensing Applications: Society and Environment, 32, 101062. https://doi.org/10.1016/j.rsase.2023.101062.

Tariq A., Siddiqui S., Sharifi A., Shah S.H.I.A. (2022). Impact of spatio-temporal land surface temperature on cropping pattern and land use and land cover changes using satellite imagery, Hafizabad District, Punjab, Province of Pakistan. Arabian Journal of Geosciences, 15, 1045. https://doi.org/10.1007/s12517-022-10238-8.

Tariq A., Yan J., Mumtaz F. (2022). Land change modeler and CA-Markov chain analysis for land use land cover change using satellite data of Peshawar, Pakistan. Physics and Chemistry of the Earth, 128, 103286. https://doi.org/10.1016/j.pce.2022.103286.

Tariq A., Mumtaz F. (2022). Modeling spatio-temporal assessment of land use land cover of Lahore and its impact on land surface temperature using multi-spectral remote sensing data. Environmental Science and Pollution Research. https://doi.org/10.1007/s11356-022-23928-3.

Tiwari A.K., Kanchan R. (2024). Analytical study on the relationship among land surface temperature, land use/land cover and spectral indices using geospatial techniques. Discover Environment, 2(1), 1. https://doi.org/10.1007/s44274-023-00021-1.

Verma P., Jangra R., Kaushik S.P. (2024). Geospatial measurement of urban sprawl and land transformation using multi-temporal datasets: A case study of Sonipat-Kundli urban agglomeration. Sustainable Environment, 10(1), 2366556. https://doi.org/10.1080/27658511.2024.2366556.

Wang M., Li M., Zhang Z., Hu T., He G., Zhang Z., Wang G., Li H., Tan J., Liu X. (2023). Land surface temperature retrieval from Landsat 9 TIRS-2 data using radiance based split-window algorithm. IEEE Journal of Selected Topics in Applied Earth Observations and Remote Sensing, 16, 1100–1113. https://doi.org/10.1109/JSTARS.2022.3232621.

Wei X., Zhang W., Zhang Z., Huang H., Meng L. (2023). Urban land use land cover classification based on GF-6 satellite imagery and multi-feature optimization. Geocarto International, 38(1), 2236579. https://doi.org/10.1080/10106049.2023.2236579.

Yuan W., Hu S., Zhan C., Wang G., Luo Y. (2025). Machine learning land surface temperature downscaling method based on Landsat 9 and Sentinel-2 satellite feature interaction. Geo-spatial Information Science. https://doi.org/10.1080/10095020.2025.2598526.

Zafar Z., Zubair M., Zha Y., Fahd S., Ahmad Nadeem A. (2024). Performance assessment of machine learning algorithms for mapping of land use/land cover using remote sensing data. Egyptian Journal of Remote Sensing and Space Science, 27(2), 216–226. https://doi.org/10.1016/j.ejrs.2024.03.003.

Zwolska A., Połrolniczak M., Kolendowicz L. (2025). Remote sensing-based analysis of urban land cover changes and surface urban heat island dynamics using Landsat and local climate zones classification in Poznan, Poland. IEEE Journal of Selected Topics in Applied Earth Observations and Remote Sensing, 18. https://doi.org/10.1109/JSTARS.2025.3583546.